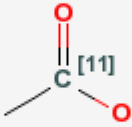


[¹¹C]Acetate

Kam Leung, PhD¹

Created: December 8, 2005; Updated: May 19, 2008.

Chemical name:	[¹¹ C]Acetate	 The image shows the chemical structure of [11C]Acetate. It consists of a central carbon atom labeled with a grey 'C' and a red '[11]' superscript. This carbon is double-bonded to an oxygen atom (red) above it and single-bonded to another oxygen atom (red) to its right. A single bond extends to the left, representing the attachment point to the rest of the molecule.
Abbreviated name:		
Synonym:	[¹¹ C]Acetic acid	
Agent Category:	Compound	
Target:	TCA cycle, fatty acid synthetase,	
Target Category:	Incorporation into membrane	
Method of detection:	PET	
Source of signal:	¹¹ C	
Activation:	No	
Studies:	<ul style="list-style-type: none">• <i>In vitro</i>• Rodents• Non-primate mammals• Non-human primates• Humans	

Click on the above structure for additional information in [PubChem](#).

¹ National Center for Biotechnology Information, NLM, NIH, Bethesda, MD; Email: micad@ncbi.nlm.nih.gov.

NLM Citation: Leung K. [¹¹C]Acetate. 2005 Dec 8 [Updated 2008 May 19]. In: Molecular Imaging and Contrast Agent Database (MICAD) [Internet]. Bethesda (MD): National Center for Biotechnology Information (US); 2004-2013.

Background

[PubMed]

Acetate is readily taken up by cells and is activated to acetyl-CoA in both the cytosol and mitochondria by acetyl-CoA synthetase. Acetyl-CoA is a common metabolic intermediate for synthesis of cholesterol and fatty acids, which are then incorporated into membrane (1). Acetyl-CoA is also oxidized in mitochondria by the tricarboxylic acid (TCA) cycle to carbon dioxide and water. Some of the acetate is converted to amino acids. In normal myocardium, acetate is metabolized to CO₂ via the TCA cycle as the dominant pathway. In contrast, tumor cells convert most of the acetate into fatty acids by a key enzyme fatty acid synthetase (FAS), which is over-expressed in cancer cells (2). Acetate is predominantly incorporated into intracellular phosphatidylcholine membrane microdomains that are important for tumor growth and metastasis (3). [¹¹C]Acetate are used as a positron emission tomography (PET) tracer for studying myocardial oxidative metabolism and regional myocardial blood flow (4). [¹¹C]Acetate is a promising PET tracer for renal, pancreatic, and prostate tumors (5).

Synthesis

[PubMed]

[¹¹C]Acetate is commonly produced by a reaction of methylmagnesium bromide or chloride and [¹¹C]carbon dioxide. This method produces [¹¹C]acetate in a radiochemical yield of 72 ± 12% in 20 min and in high specific activity (>18.5 GBq/μmol, 0.5 Ci/μmol). The radiochemical purity of [¹¹C]acetate was found to be > 95% (6). Several automated systems provided radiochemical yields of 60 - 80% and radiochemical purity of 99% in 15 - 23 min (7-9)

In Vitro Studies: Testing in Cells and Tissues

[PubMed]

Acetate uptake and metabolism were studied in four tumor cell lines and one fibroblast cell line with [¹⁴C]acetate. All four tumor cell lines showed higher accumulation of [¹⁴C] activity than the resting fibroblasts. Tumor-to-fibroblast ratios were larger than those of [³H]-2-deoxyglucose. [¹⁴C]Acetate was metabolized and incorporated into phosphatidylcholine and neutral lipids in proportionally to cellular proliferation rates. The remaining fraction of [¹⁴C]acetate was converted to amino acids, acetylCoA, and CO₂ (10). This was shown by extraction of tissue samples followed by analysis using thin layer chromatography and paper chromatography with authentic samples of possible metabolites.

Animal Studies

Rodents

[PubMed]

Tissue accumulation of $[^{11}\text{C}]$ acetate was studied in mice with EMT-6 murine mammary carcinoma tumors and rats with 9L-glioma tumors at 1 h postinjection of the tracer (11). In the EMT-6 mice, the organ with the highest uptake was in the pancreas (2.49% injected dose/g (ID/g)), followed by the liver (1.42% ID/g), spleen (1.40% ID/g) and kidneys (1.18% ID/g). The tumor uptake was only 0.60% ID/g giving a tumor-to-blood ratio of 1.3. In the rats bearing 9L-glioma tumors, the organ with the highest uptake was in the pancreas (0.88% ID/g), followed by the spleen (0.42% ID/g), liver (0.35% ID/g), and kidneys (0.33% ID/g). The tumor uptake was only 0.42% ID/g giving a tumor-to-blood ratio of 3.2.

Oyama et al. reported that androgen ablation caused a decrease of 2- $[^{18}\text{F}]$ fluoro-2-deoxy-D-glucose ($[^{18}\text{F}]$ FDG) and $[^{11}\text{C}]$ acetate uptake in the prostate in Sprague-Dawley male rats to monitor metabolic changes in normal prostate tissue. Dihydrotestosterone administration returned uptake of both tracers to that of the baseline level. Therefore, serum testosterone levels influence glucose and acetate metabolism in the prostate (12).

$[^{11}\text{C}]$ Acetate has been used to study myocardial oxygen consumption rate (MVO_2) with the metabolic fate of the tracer in normoxic, hypoxic, and ischemic conditions in isolated perfused rat hearts. Model-estimated MVO_2 correlated well with experimentally measured MVO_2 for these conditions correlated strongly with the myocardial clearance rate determined from the tissue kinetics (13).

In a rat model of an occluded, acute left anterior descending (LAD) coronary artery, ^{60}Cu -ATSM was used to visualize hypoxic rat heart tissue using an *ex vivo* tissue slice imaging technique (14). In addition, $[^{11}\text{C}]$ acetate was used to monitor myocardial blood flow. Low $[^{11}\text{C}]$ acetate uptake (low blood flow) and high ^{60}Cu -ATSM uptake (hypoxia) were observed in mildly ischemic regions. In the center of severely ischemic regions with no blood flow, little accumulation of ^{11}C or ^{60}Cu radioactivity was observed.

Other Non-Primate Mammals

[PubMed]

$[^{11}\text{C}]$ Acetate PET was used to study cardiac output in a pig model (15). The tracer uptake in the right and left heart cavities was measured as well as in the lung. Myocardial output measured by $[^{11}\text{C}]$ acetate PET was linearly related to cardiac output by thermodilution. Lung uptake of $[^{11}\text{C}]$ acetate was also linearly related to stroke volume.

Non-Human Primates

[PubMed]

[¹¹C]Acetate PET was studied in monkeys with coronary ligation. The infarct myocardial regions showed a decrease in tracer accumulation (16).

Human Studies

[PubMed]

Myocardial oxygen consumption can be estimated with PET from analysis of the myocardial turnover rate constant (k) after administration of [¹¹C]acetate. [¹¹C]Acetate was administered to five normal volunteers and six patients with myocardial infarction. Uptake of [¹¹C]acetate by the myocardium was avid, and its clearance from the blood pool was rapid, yielding myocardial images of excellent quality. Regional k was homogeneous in the myocardiums of healthy volunteers. In patients, k in regions remote from the area of infarction was not different from values in the myocardiums of healthy human volunteers. In contrast, k in the center of the infarct region of necrotic myocardium was significantly reduced (17).

[¹¹C]Acetate PET has been shown to have high sensitivity for detection of recurrent prostate cancer and metastases. It was reported that 27 of 46 prostate cancer patients were positive with [¹¹C]acetate PET studies, whereas only eight [¹⁸F]FDG PET studies had positive detections (18). In another study, it was cautioned that acetate also accumulates in normal, hyperplastic, and benign prostate tissues. It was reported that the [¹¹C]acetate standardized uptake values for normal prostate and benign prostate, overlap significantly with those for prostate cancer patients (19).

Human dosimetry was estimated in six healthy volunteers by intravenous injection of 525 MBq (14.2 mCi) of [¹¹C]acetate (20). The organs receiving the highest absorbed doses were the pancreas (0.017 mGy/MBq or 62.9 mrad/mCi), bowel (0.011 mGy/MBq or 40.7 mrad/mCi), kidneys (0.0092 mGy/MBq or 34.0 mrad/mCi), and spleen (0.0092 mGy/MBq or 34.0 mrad/mCi). No urinary excretion of tracer was detected. The effective dose equivalent was 0.0062 mSv/MBq (22.9 mrem/mCi).

[¹¹C]Acetate is rapidly taken up by myocardium and metabolized to CO₂ and water after intravenous injection. The uptake is indirectly dependent on blood flow (21). The clearance of the tracer is a direct reflection of TCA cycle activity, which is coupled to myocardial oxygen consumption [PubMed]. Rates of clearance from myocardium of [¹¹C]acetate reflect oxidative metabolism (22). [¹¹C]Acetate PET is used to evaluate ischemia and myocardial infarction [PubMed]. Many prostate, bladder, and renal cancer patients have been imaged with [¹¹C]acetate PET to assess primary and metastatic tumors [PubMed].

NIH Support

HL13851, P30 CA91842, R24 CA83060, HL29845, HL33177, HL17646, R01 HL46895, R01 HL58408, RR00645

References

1. Howard B.V., Howard W.J. Lipids in normal and tumor cells in culture. *Prog Biochem Pharmacol.* 1975;**10**:135–66. PubMed PMID: 1093205.
2. Swinnen J.V., Heemers H., Deboel L., Fougelle F., Heyns W., Verhoeven G. Stimulation of tumor-associated fatty acid synthase expression by growth factor activation of the sterol regulatory element-binding protein pathway. *Oncogene.* 2000;**19**(45):5173–81. PubMed PMID: 11064454.
3. Swinnen J.V., Van Veldhoven P.P., Timmermans L., De Schrijver E., Brusselmans K., Vanderhoydonc F., Van de Sande T., Heemers H., Heyns W., Verhoeven G. Fatty acid synthase drives the synthesis of phospholipids partitioning into detergent-resistant membrane microdomains. *Biochem Biophys Res Commun.* 2003;**302**(4):898–903. PubMed PMID: 12646257.
4. Visser F.C. Imaging of cardiac metabolism using radiolabelled glucose, fatty acids and acetate. *Coron Artery Dis.* 2001;**12Suppl 1S**12–8. PubMed PMID: 11286301.
5. Schoder H., Larson S.M. Positron emission tomography for prostate, bladder, and renal cancer. *Semin Nucl Med.* 2004;**34**(4):274–92. PubMed PMID: 15493005.
6. Pike V.W., Eakins M.N., Allan R.M., Selwyn A.P. Preparation of [1-¹¹C]acetate--an agent for the study of myocardial metabolism by positron emission tomography. *Int J Appl Radiat Isot.* 1982;**33**(7):505–12. PubMed PMID: 6981606.
7. Kruijer P.S., Ter Linden T., Mooij R., Visser F.C., Herscheid J.D.M. A practical method for the preparation of [¹¹C]acetate. *Appl. Radiat. Isot.* 1995;**46**:317–321.
8. Moerlein S.M., Gaehle G.G., Welch M.J. Robotic preparation of Sodium Acetate C 11 Injection for use in clinical PET. *Nucl Med Biol.* 2002;**29**(5):613–21. PubMed PMID: 12088733.
9. Roeda D., Dolle F., Crouzel C. An improvement of ¹¹C acetate synthesis--non-radioactive contaminants by irradiation-induced species emanating from the ¹¹C carbon dioxide production target. *Appl Radiat Isot.* 2002;**57**(6):857–60. PubMed PMID: 12406629.
10. Yoshimoto M., Waki A., Yonekura Y., Sadato N., Murata T., Omata N., Takahashi N., Welch M.J., Fujibayashi Y. Characterization of acetate metabolism in tumor cells in relation to cell proliferation: acetate metabolism in tumor cells. *Nucl Med Biol.* 2001;**28**(2):117–22. PubMed PMID: 11295421.
11. Jonson S.D., Welch M.J. Investigations into tumor accumulation and peroxisome proliferator activated receptor binding by F-18 and C-11 fatty acids. *Nucl Med Biol.* 2002;**29**(2):211–6. PubMed PMID: 11823126.
12. Oyama N., Kim J., Jones L.A., Mercer N.M., Engelbach J.A., Sharp T.L., Welch M.J. MicroPET assessment of androgenic control of glucose and acetate uptake in the rat prostate and a prostate cancer tumor model. *Nucl Med Biol.* 2002;**29**(8):783–90. PubMed PMID: 12453586.
13. Ng C.K., Huang S.C., Schelbert H.R., Buxton D.B. Validation of a model for [1-¹¹C]acetate as a tracer of cardiac oxidative metabolism. *Am J Physiol.* 1994;**266**(4 Pt 2):H1304–15. PubMed PMID: 8184908.

14. Fujibayashi Y., Cutler C.S., Anderson C.J., McCarthy D.W., Jones L.A., Sharp T., Yonekura Y., Welch M.J. Comparative studies of Cu-64-ATSM and C-11-acetate in an acute myocardial infarction model: ex vivo imaging of hypoxia in rats. *Nucl Med Biol.* 1999;**26**(1):117–21. PubMed PMID: 10096511.
15. Sorensen J., Stahle E., Langstrom B., Frostfeldt G., Wikstrom G., Hedenstierna G. Simple and accurate assessment of forward cardiac output by use of 1-(11)C-acetate PET verified in a pig model. *J Nucl Med.* 2003;**44**(7):1176–83. PubMed PMID: 12843234.
16. Norol F., Merlet P., Isnard R., Sebillon P., Bonnet N., Cailliot C., Carrion C., Ribeiro M., Charlotte F., Pradeau P., Mayol J.F., Peinnequin A., Drouet M., Safsafi K., Vernant J.P., Herodin F. Influence of mobilized stem cells on myocardial infarct repair in a nonhuman primate model. *Blood.* 2003;**102**(13):4361–8. PubMed PMID: 12947003.
17. Walsh M.N., Geltman E.M., Brown M.A., Henes C.G., Weinheimer C.J., Sobel B.E., Bergmann S.R. Noninvasive estimation of regional myocardial oxygen consumption by positron emission tomography with carbon-11 acetate in patients with myocardial infarction. *J Nucl Med.* 1989;**30**(11):1798–808. PubMed PMID: 2809744.
18. Oyama N., Miller T.R., Dehdashti F., Siegel B.A., Fischer K.C., Michalski J.M., Kibel A.S., Andriole G.L., Picus J., Welch M.J. 11C-acetate PET imaging of prostate cancer: detection of recurrent disease at PSA relapse. *J Nucl Med.* 2003;**44**(4):549–55. PubMed PMID: 12679398.
19. Kato T., Tsukamoto E., Kuge Y., Takei T., Shiga T., Shinohara N., Katoh C., Nakada K., Tamaki N. Accumulation of [11C]acetate in normal prostate and benign prostatic hyperplasia: comparison with prostate cancer. *Eur J Nucl Med Mol Imaging.* 2002;**29**(11):1492–5. PubMed PMID: 12397469.
20. Seltzer M.A., Jahan S.A., Sparks R., Stout D.B., Satyamurthy N., Dahlbom M., Phelps M.E., Barrio J.R. Radiation dose estimates in humans for (11)C-acetate whole-body PET. *J Nucl Med.* 2004;**45**(7):1233–6. PubMed PMID: 15235071.
21. Gropler R.J., Siegel B.A., Geltman E.M. Myocardial uptake of carbon-11-acetate as an indirect estimate of regional myocardial blood flow. *J Nucl Med.* 1991;**32**(2):245–51. PubMed PMID: 1992027.
22. Sciacca R.R., Akinboboye O., Chou R.L., Epstein S., Bergmann S.R. Measurement of myocardial blood flow with PET using 1-11C-acetate. *J Nucl Med.* 2001;**42**(1):63–70. PubMed PMID: 11197982.